Fluorescence of Photochromic 1,2-Bis(3-methyl-2-thienyl)ethene

Tuyoshi Fukaminato, Tsuyoshi Kawai,* Seiya Kobatake, and Masahiro Irie*

Department of Chemistry and Biochemistry, Graduate School of Engineering, Kyushu University, Hakozaki 6-10-1, Higashi-ku, Fukuoka 812-8581, Japan

Received: March 12, 2003; In Final Form: May 31, 2003

Characteristic fluorescence properties of photochromic 1,2-bis(3-methyl-2-thienyl)perfluorocyclopentene were studied in solution as well as in the single-crystalline phase. When the concentration of 1,2-bis(3-methyl-2-thienyl)perfluorocyclopentene was increased in a 3-methylpentane solution, the fluorescence spectrum showed a bathochromic shift and a new fluorescence excitation peak attributable to intermolecular aggregates was observed in the wavelength region between 350 and 400 nm. Upon irradiation with light shorter than 330 nm, the dithienylethene derivatives underwent a photochromic reaction to produce the closed-ring isomer, while no reaction was observed when excited at 350−400 nm. Similar fluorescence spectra attributable to intermolecular interaction were observed in the spectrum of the single crystal. X-ray crystallographic analysis and polarized fluorescence measurement revealed that the characteristic photochromic reactivity and fluorescence property are controlled by the intermolecular interaction between two neighboring thiophene rings.

Introduction

Organic photochromic materials have attracted much attention because of their potential application to optical memory media and optical switches.[1−4] Among various types of photochromic compounds,[5,6] diarylethene derivatives[7,8] are the most promising because of their excellent thermal stability in both isomers,[9,10] fatigue resistant character,[11,12] rapid response,[13−16] and high reactivity in the solid state.[17,18] Diarylethene derivatives undergo cyclization/cycloreversion reactions. Depending on the substitution position of thiophene to the ethene moiety there exist two types of diarylethene derivatives, as shown in Scheme 1. So far, bis(3-thienyl)ethene-type diarylethenes have been extensively studied, whereas only a few studies have been carried out concerning bis(2-thienyl)ethene-type derivatives.[19−23] Bis(2-thienyl)ethene derivatives have the following characteristic features; (1) the π-conjugation extends throughout the molecule in the open-ring isomer, while it is localized in the central cyclohexadiene in the closed-ring isomer, (2) the absorption spectrum of the closed-ring isomer shifts to a shorter wavelength in comparison with that of bis(3-thienyl)ethene derivatives, and (3) the open-ring isomer exhibits appreciable fluorescence.

Recently, we have demonstrated three-dimensional optical recording in a single crystal of 1,2-bis(3-methyl-2-thienyl)-perfluorocyclopentene (**1**) (Scheme 2), the recorded information being detected with use of fluorescence.[24] However, the fundamental fluorescence properties of bis(2-thienyl)ethene-type derivatives have not yet been studied in detail. In this paper, we report on fluorescence properties of **1** in solution as well as in the single-crystalline phase at room temperature and 77 K.

SCHEME 1

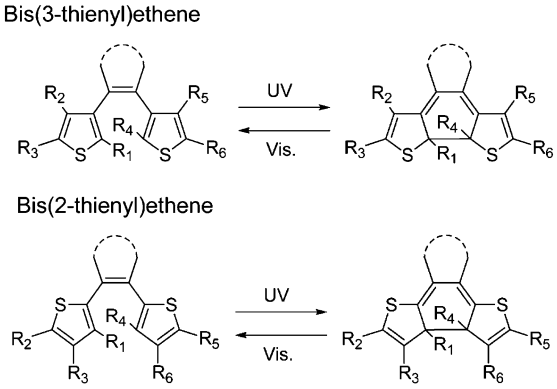

SCHEME 2

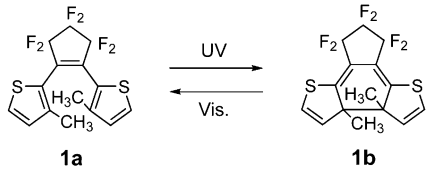

Experimental Section

A detailed synthetic procedure of **1** has already been reported.[24] The solvents used were spectroscopic grade and purified by distillation before use. ^{1}H NMR spectra were recorded on a Varian Gemini 200 spectrometer (200 MHz). Tetramethylsilane was used as an internal standard. Absorption and fluorescence spectra in solution were measured with a Hitachi U-3410 absorption spectrophotometer and a Hitachi F-3010 fluorescence spectrophotometer, respectively. Fluorescence emission and excitation spectra were corrected by using acridine yellow and acridine orange as the reference. Photoirradiation was carried out with an USHIO 500 W high-pressure mercury lamp or an USHIO 500 W xenon lamp as the light sources. Monochromic light was obtained by passing the light through a monochromator (Ritsu MV-10N) or a band-pass filter ($\Delta\lambda_{1/2} = 15$ nm). The cyclization and cycloreversion quantum yields were determined by comparing the reaction rates of

* Address correspondence to these authors. E-mail: irie@cstf.kyushu-u.ac.jp; tkawai@cstf.kyushu-u.ac.jp. Phone: +81-92-642-3556. Fax: +81-92-642-3568.

10.1021/jp034624d CCC: $25.00
Published on Web 07/11/2003

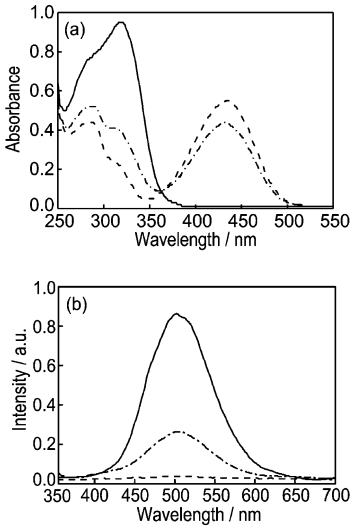

Figure 1. (a) Absorption and (b) fluorescence spectral changes of **1** in 3-methylpentane at room temperature: open-ring isomer **1a** (—), photostationary state (-·-), and closed-ring isomer **1b** (- - -). The concentration of **1** in 3-methylpentane was 8.0×10^{-5} M.

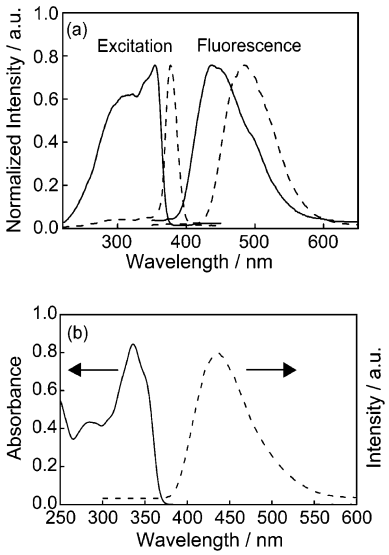

Figure 2. (a) Fluorescence and excitation spectra of **1a** (10^{-2} M) in 3-methylpentane at 77 K. Excitation wavelength for the fluorescence spectra: 313 nm (—), 386 nm (- - -). Monitoring wavelength for the excitation spectra: 400 nm (—), 550 nm (- - -). (b) Absorption (—) and fluorescence (- - -) spectra of **1a** (10^{-5} M) in 3-methylpentane at 77 K.

furylfulgide in hexane, using the well-established procedure.[25,26] Absorption and fluorescence spectra in the single-crystalline phase were measured by using a Leica DMLP or a JASCO MICRO-20 polarizing microscope connected with a Hamamatsu PMA-11 photodetector. A xenon lamp (75 W) and a halogen lamp (100 W) were used as the light sources to induce reactions in crystals. The wavelength of the light was selected by passing the light through a band-pass filter. For the low-temperature measurements of optical properties, an Oxford DN 1015 cryostat was used.

Fluorescence lifetime was measured with a time-resolved spectrofluorometer (Hamamatsu Photonics C4334-01, C5094, and C4792) excited with a pulsed N_2 laser and a dye laser system (Laser Photonics, Inc., LN-203C and LD2S). The pulse width was 600 ps and the wavelengths were 337.1 (N_2 laser) and 386.5/400 nm (dye laser). The decay curves were analyzed with the single-exponential or the multi-exponential fitting after deconvolution of the excitation light pulse profile. The goodness of the fit was judged with the reduced χ^2 value (<1.2 in all cases), the randomness of the residuals, and the autocorrelation function.

X-ray crystallographic analysis was carried out with a Bruker SMART CCD diffractometer.

Results and Discussion

Photochromism and Fluorescence in Solution. Figure 1 shows typical absorption and fluorescence spectra of **1a** (8×10^{-5} M) in 3-methylpentane. The absorption maximum of **1a** was observed at 316 nm ($\epsilon = 1.2 \times 10^4$ M^{-1} cm^{-1}; 1 M = 1 mol dm^{-3}). Upon irradiation with 313-nm light, the colorless 3-methylpentane solution of **1a** turned yellow, in which the absorption maximum was observed at 432 nm ($\epsilon = 6.87 \times 10^3$ M^{-1} cm^{-1}). The colored isomer **1b** was stable and could be isolated by HPLC. The absorption spectrum of **1b** is also shown in Figure 1. The yellow solution returned to a colorless one upon irradiation with visible light (λ > 450 nm). The quantum yields of cyclization and cycloreversion reactions of **1** were determined in 3-methylpentane solution to be 0.54 (313 nm) and 0.37 (432 nm) at room temperature, respectively.

1a exhibited fluorescence at 500 nm in 3-methylpentane solution (8×10^{-5} M) when excited at 313 nm. The fluorescence intensity decreased along with the photochromism from **1a** to **1b** upon irradiation with 313 nm light, as shown in Figure 1b. The isolated closed-ring isomer **1b** did not show any fluorescence. The fluorescence quantum yield of **1a** in 3-methylpentane solution was measured using anthracene ($\Phi_f = 0.29$) as a reference and determined to be 0.01. It should be noted that the Stokes shift of the fluorescence is relatively large and the fluorescence spectral edge showed a red-shift in comparison with the absorption edge. The origin of this large Stokes shift has already been discussed in detail by Sekiya et al.[27]

(a) Concentration Dependence of Fluorescence Spectra at Room Temperature and 77 K. Panels a and b in Figure 2 show the fluorescence and excitation spectra at 77 K at the concentrations of 10^{-2} and 10^{-5} M, respectively. When a high-concentration solution (10^{-2} M) was excited at 313 nm, an emission peak was observed at 440 nm (solid line in Figure 2a). The peak position agreed with the position observed at low concentration (<10^{-5} M) shown by the broken line in Figure 2b. On the other hand, a new fluorescence emission maximum was observed at 490 nm with excitation at 386 nm, as shown by the broken line in Figure 2a. The excitation spectra of these two fluorescence spectra were completely different as shown in Figure 2a. The excitation spectrum for the 550-nm emission showed a clear peak at 380 nm (broken line in Figure 2a), while the spectrum for the 400-nm emission showed a broad band between 250 and 360 nm (solid line in Figure 2a).

The concentration dependence of fluorescence excitation spectra was measured in 3-methylpentane solution at room temperature and 77 K, as shown in Figure 3. The fluorescence excitation spectra showed remarkable concentration dependence. The excitation spectrum at room temperature was composed of two bands at 300 and 360 nm, and the latter was observed only in the solution containing **1a** at a concentration higher than 10^{-5} M. At 77 K, the fluorescence excitation spectra showed a systematic red shift with an increase in concentration. These results indicate that molecular aggregation, which is frequently observed in π-conjugated molecules such as oligothiophene,[28,29] poly(phenyleneethynylene)s,[30−37] and other arylethynyl fluorophores,[38] takes place in 3-methylpentane and the excitation

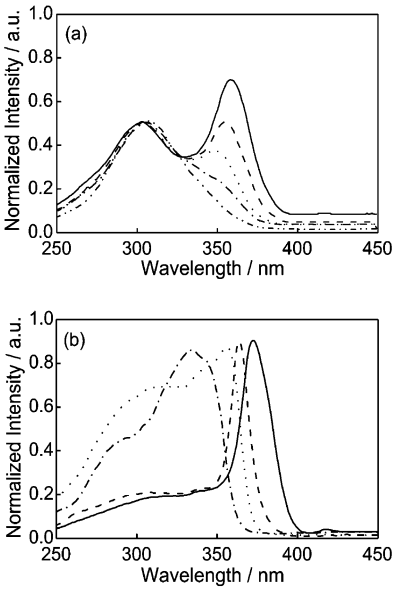

Figure 3. Fluorescence excitation spectra of **1a** in 3-methylpentane: (a) at room temperature, monitored at 500 nm; and (b) at 77 K, monitored at 450 nm. The concentrations of **1a** were 10^{-2} (—), 10^{-3} (- - -), 10^{-4} (• • •), 10^{-5} (- • -), and 10^{-6} M (- • • -).

spectra at around 360 nm are due to the band of the aggregates. The gradual red peak shift with an increase in the concentration at 77 K suggests the existence of various types of aggregates. No concentration effect was discerned in the UV−vis absorption spectrum, or in the ^{1}H NMR spectrum. These results suggest that the total amount of the aggregates is very small and the fluorescence quantum yield of the aggregates is markedly higher than that of the monomer.

The lifetimes of the two components were measured with a time-resolved fluorescence spectrometer at low temperature (77 K). Figure 4a shows the fluorescence decay curve at 10^{-2} M with different excitation wavelengths at 337 and 386 nm. The decay curves of the two components were clearly observed with excitation at 337 nm. The lifetimes of the two components were evaluated to be less than 0.5 and 6.4 ns, respectively. The fluorescence maximum of the short-lifetime component was observed at 435 nm and that of long-lifetime component at 487 nm, as shown in Figure 4b. On the other hand, a single-exponential decay curve was observed with excitation at 386 nm. The fluorescence spectra remained the same during the lifetime, as shown in Figure 4c. The lifetime was evaluated to be 6.3 ns, which agreed well with that of the longer lifetime component excited at 337 nm (Figure 4a). These results indicate that two or more chemical species are excited with 337-nm light, while 386-nm light excites only one species with a longer lifetime and a longer emission wavelength. These transient emission behaviors are consistent with the results of CW fluorescence emissions shown in Figures 2 and 3.

Similar time-resolved fluorescence measurement was carried out for a very low concentration solution at 77 K. Figure 5a shows the fluorescence decay curve at 10^{-6} M excited at 337 nm. The lifetime was evaluated to be less than 0.5 ns, and the fluorescence maximum remained the same at 435 nm during the lifetime, as shown in Figure 5b. The peak wavelength agrees with that in the spectrum of the short-lifetime component of Figure 4a. This means that the short-lifetime fluorescence component is possibly assigned to the monomer emission and the long-lifetime fluorescence component is ascribed to the intermolecular aggregates having a large fluorescence quantum yield.

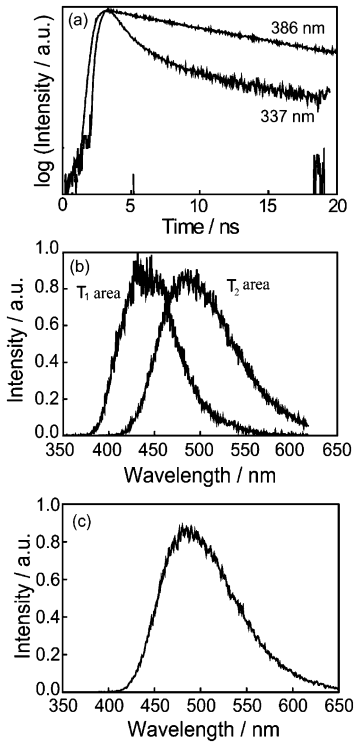

Figure 4. (a) Time-resolved fluorescence decay curves of **1a** (10^{-2} M) in 3-methylpentane at 77 K. Under excitation with 337 and 386 nm light. (b) Fluorescence spectra in the time domains of T_1 (0−1.0 ns) and T_2 (1.0−20 ns) excited at 337 nm light. (c) Fluorescence spectra of the high-concentration solution (10^{-2} M) excited at 386-nm light.

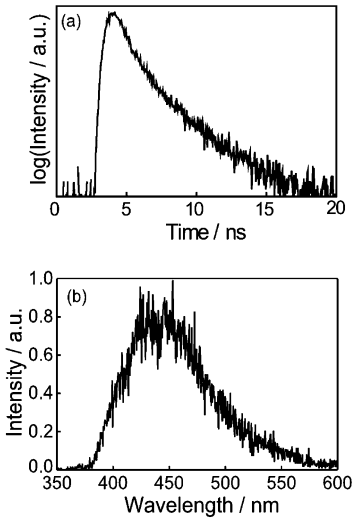

Figure 5. (a) Time-resolved fluorescence decay curves of **1a** (10^{-6} M) in 3-methylpentane at 77 K. Under excitation with 337-nm light. (b) Fluorescence spectra of the low concentration solution (10^{-6} M) excited at 337-nm light.

(b) Excitation Wavelength Dependence of Photochromism. It is inferred from the above results that more than two fluorescence components exist in the ground state and their fluorescence properties depend on the excitation wavelength when the concentration is high (10^{-2} M). This suggests that the photochromic behavior is also dependent on the excitation wavelength at high concentration. The excitation wavelength dependence of the photocyclization reactivity was measured by irradiation with 313- and 386-nm light. When irradiated with 313-nm light for 10 s, the colorless 3-methylpentane solution changed to yellow. On the other hand, when irradiated with 386-nm light, no color change was observed even after

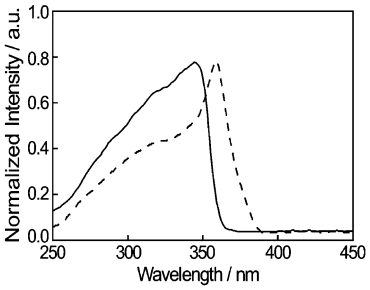

Figure 6. Fluorescence excitation spectra of **1a** (10^{-4} M) monitored at 450 nm in MTHF at 77 K; the excitation spectrum of the sample, which was prepared by photobleaching **1b** at 77 K (−), The excitation spectra of the above sample, which was warmed to room temperature and then frozen at 77 K (- - -).

TABLE 1: Spectroscopic Properties, Quantum Yields, and Fluorescence Decay Times of 1a at Room Temperature in Various Solutions at 10^{-6} M

solvent	λ_{max} (nm)[a]	λ_{max} (nm)[b]	λ_{max} (nm)[c]	Φ_f[d]	τ_1 (ns)[e]	τ_2 (ns)[e]	A_1/A_2
3-methylpentane	316	306	500	1.0	<0.5	5.68	88/12
2-methyl-THF	325	311	516	0.69	<0.5	4.29	90/10
CH_3CN	326	311	518	0.51	<0.5	2.87	90/10

[a] Absorption maxima. [b] Excitation maxima. Emission wavelength: 500 nm. [c] Fluorescence maxima. Excitation wavelength: 313 nm. [d] Relative fluorescence quantum yield. Excitation wavelength: 313 nm. [e] Fluorescence decay times. Excitation wavelength: 337 nm.

prolonged irradiation for 10 h. Since the absorption intensity at 386 nm is about 5% of that at 313 nm, the difference in the reactivity indicates that the photochromic reaction quantum yield of the aggregate is at least less than 0.003.

The π-conjugation extends over the molecule in the open-ring isomer (**1a**), whereas the π-conjugation is localized in the central cyclohexadiene in the closed-ring isomer (**1b**), as described above. The difference in the π-conjugation length is considered to affect the intermolecular interaction. The solid line of Figure 6 shows the fluorescence excitation spectra of **1a**, which was prepared by photocycloreversion reaction of **1b** in 2-methyltetrahydrofuran (MTHF) by irradiation with visible light irradiation at 77 K (the solid line in Figure 6). The excitation spectrum agreed well with the spectrum of the very dilute solution (dotted line) as shown in Figure 3b. This indicates that **1a** molecules are molecularly dispersed in the frozen solution. The sample was warmed to room temperature and then frozen again at 77 K. Then the excitation spectrum was measured. The characteristic excitation peak at 370 nm was observed. These results indicate that **1a** molecules aggregated in the melted solution. The intermolecular interaction is a characteristic feature of **1a** molecules and different from that of **1b** molecules. This result clearly indicates that the aggregation takes place among **1a** molecules, which has extended the π-conjugation system over both thiophene rings of the molecule.

The solvent effect on the fluorescence spectra was also studied to exclude the contribution of TICT (Twisted Intramolecular Charge Transfer).[39−42] Table 1 summarizes the absorption, excitation, and fluorescence maxima, the fluorescence quantum yields, and the fluorescence lifetimes of **1a** in various solvents. Although the fluorescence quantum yields and the fluorescence lifetimes of **1a** decreased with an increase in solvent polarity, the solvent effect was not significant. The fluorescence maximum was observed between 500 and 520 nm in all solvents, and solvent polarity did not affect the ratio of two fluorescence decay components. These results exclude the contribution of the TICT effect on the fluorescence spectrum.

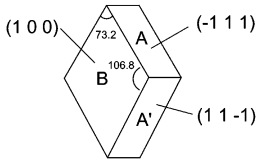

Figure 7. The shape a single crystal of **1a**.

TABLE 2: Crystal Data and Structure Refinement for 1a

	1a
formula	$C_{15}H_{10}F_6S_2$
fw	368.35
temp/K	296(2)
cryst system	monoclinic
space group	*C*2/*c*
unit cell dimens.	
a/Å	18.311(8)
b/Å	8.706(4)
c/Å	11.720(5)
α/deg	90
β/deg	121.962(6)
γ/deg	90
V/Å^3	1585.0(12)
Z	4
D_{calcd}/(g/cm^3)	1.544
final *R* indices [$I > 2\sigma(I)$]	
*R*1	0.0347
*wR*2	0.0910
R indices (all data)	
*R*1	0.0496
*wR*2	0.0990

Photochromism and Fluorescence in Single Crystals. A rhombus-shaped single crystal was obtained by recrystallization of **1a** from hexane solution as illustrated in Figure 7. The crystal consists of six surfaces with four rectangles (A and A′) and two parallelograms (B). Table 2 shows the results of the X-ray crystallographic analysis of **1a**. The ORTEP drawing of **1a** indicates that **1a** is packed in photoactive antiparallel conformation with C_2 symmetry in the crystal. The distance between the reacting carbon atoms was measured to be 3.62 Å, which is short enough for the reaction.[18] The planes of {(1−1−1), (−1 1 1)} and {(1 1−1), (−1−1 1)} correspond to surfaces A and A′, respectively, and the planes of {(1 0 0), (−1 0 0)} correspond to surface B. All the following measurements were carried out with use of surface A.

(a) Fluorescence Characteristics. Figure 8 shows the absorption, fluorescence excitation, and fluorescence spectra of a single crystal of **1a** at room temperature. When excited at 366 nm, the fluorescence maximum was observed at 520 nm, which is about 20 nm longer than that in very dilute hexane solution. The fluorescence excitation spectra monitored at 520 nm was observed between 370 and 450 nm. The peak wavelength of the excitation bands roughly agreed with the wavelength of a shoulder in the absorption band at 400 nm. Figure 8b shows the wavelength dependence of the fluorescence and excitation spectra of **1a** in the single crystal at 77 K. When excited at 313 nm, the fluorescence maximum was observed at 500 nm with a shoulder around 430 nm (solid line). On the other hand, only one peak was observed at 500 nm with excitation at 400 nm (broken line). The fluorescence excitation spectra monitored at 500 nm exhibited the characteristic excitation band at about 400 nm, while a broad excitation band around 350 nm was observed when monitored at 430 nm (solid line). This fluorescence behavior is very similar to that observed for the high-concentration sample at 77 K.

The two fluorescence components observed in the single-crystalline phase at low temperature were characterized by time-

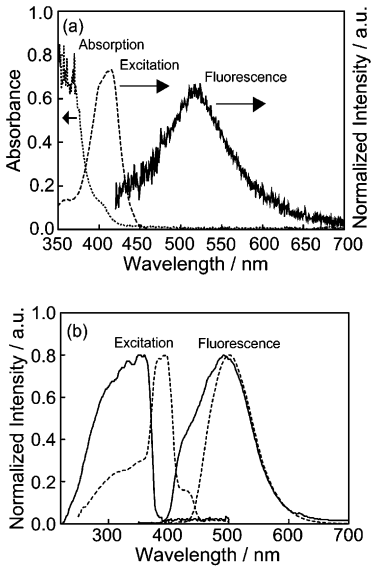

Figure 8. (a) Absorption (• • •), fluorescence excitation (- - -), and fluorescence (−) spectra of a single crystal of **1a**. The fluorescence excitation spectrum was monitored at 500 nm. The excitation wavelength was 366 nm. (b) Fluorescence emission and excitation spectra of a single crystal of **1a** at 77 K excited at 313 (−) and 400 nm (- - -) and monitored at 430 nm (−) and 550 nm (- - -).

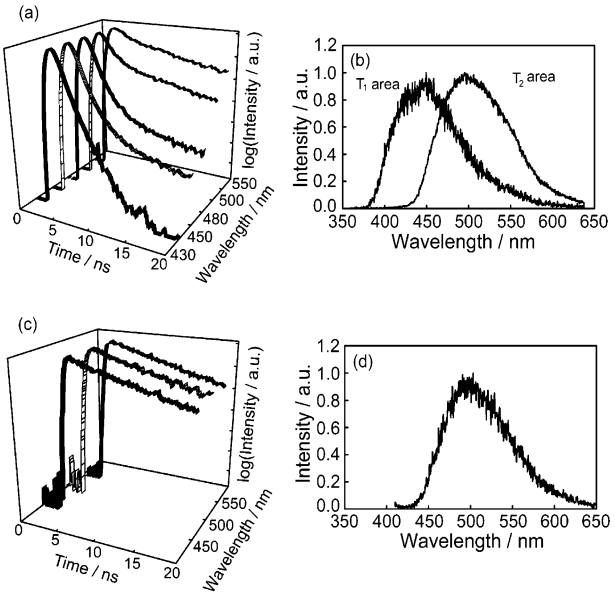

Figure 9. (a) Time-resolved fluorescence decay curves of a single crystal of **1a** at 77 K excited at 337 nm. (b) Fluorescence spectra in the time domains of T_1 (0−1.0 ns) and T_2 (1.0−20 ns). (c) Time-resolved fluorescence decay curves of a single crystal of **1a** at 77 K excited at 386 nm. (d) Fluorescence spectra.

resolved fluorescence measurement with different excitation wavelengths. Panels a and c in Figure 9 show the monitoring wavelength dependence of the fluorescence decay curves with different excitation wavelengths (panel a, 337 nm; panel c, 400 nm). When excited at 337 nm, the fluorescence decay of **1a** followed multiexponentials expression. When analyzed with two exponential decays, the lifetimes were evaluated to be less than 0.81 and 9.23 ns. Figure 9b shows the fluorescence spectra ofthe short-lifetime component (0 ns < T_1 < 1.0 ns) and the long-lifetime component (1.0 ns < T_2 < 20 ns). The fluorescence maxima of the short-lifetime and long-lifetime components were observed at 435 and 495 nm, respectively (Figure 9b). On the other hand, single-exponential decay curves were observed when excited at 400 nm, as shown in Figure 9c. The fluorescence

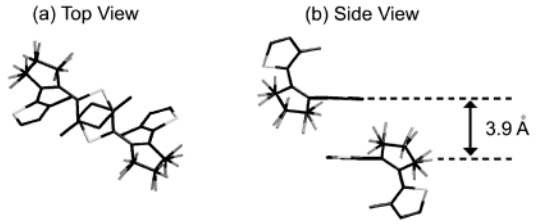

Figure 10. Sectional views of neighboring **1a** molecules: (a) top view and (b) side view.

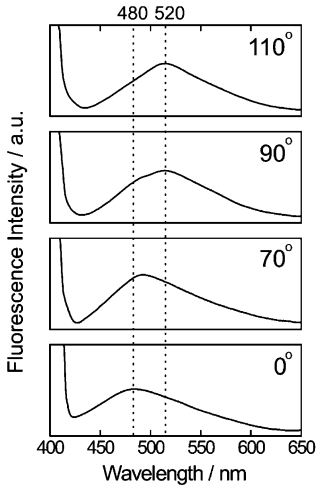

Figure 11. Polarized fluorescence spectra of a single crystal of **1a** excited at 366 nm.

spectrum remained the same in all time domains, as shown in Figure 9d. The lifetime was evaluated to be 9.36 ns. These results indicate that two or more components are excited with 337-nm light, while 400-nm light excites only one component with a longer lifetime and a longer emission wavelength maximum. The lifetime behavior is also similar to the results observed in the high-concentration solution.

(b) Photochromism. Colorless single-crystal **1a** turned yellow upon irradiation with UV (366 nm) light. The yellow color of the crystal is due to the formation of **1b**. The yellow color of the crystal disappeared upon irradiation with visible light (λ > 450 nm). The photochromic reactivity depended on the excitation wavelength, as observed in the high-concentration solution. Upon irradiation with 313-nm light for 10 s, the colorless crystal turned yellow. On the other hand, when excited at 400 nm, where the crystal still has appreciable absorption, no color change was observed even after irradiation for 10 h.

Figure 10 shows the sectional view of the adjacent molecules in a single crystal of **1a**. In the crystal two thiophene rings of the adjacent molecules have parallel face-to-face stacking and the center-to-center distance between the two thiophene rings of the adjacent molecules was about 3.9 Å, which is short enough for $\pi-\pi$ intermolecular interaction. Figure 11 shows the polarized fluorescence spectra of the crystal. Nonpolarized light was used as the excitation light and the fluorescence of a particular direction was collected by setting an analyzer in front of the detector. The fluorescence maximum and intensity varied depending on the detection polarization angle. The fluorescence maximum was observed at around 480 nm at a certain angel (0°), while the maximum shifted to 520 nm when detected at 90°. It should be noted that the fluorescence spectra were not the same when monitored at 70° and at 110°. At 70°, 480 nm emission was observed, while 520 nm emission dominated when detected at 110°. Two or more transition dipole moments which contribute to the fluorescence should exist in the crystal of **1a**.

The longer wavelength emission is considered to be attributed to the intermolecular interaction, whose polarization direction differs from that of the monomer molecule.

Conclusion

Fluorescence characteristics of 1,2-bis(3-methyl-2-thienyl)-perfluorocyclopentene (**1**) in solution as well as in the single-crystalline phase were studied by CW fluorescence spectra, time-resolved fluorescence spectra, and X-ray crystallographic analysis. When the concentration of **1a** was increased in solution, a new fluorescence excitation peak, which is ascribed to the intermolecular aggregates, was observed in the wavelength region between 350 and 400 nm. In the high-concentration solution, when excited at a wavelength shorter than 330 nm, **1a** underwent photochromic reaction to **1b**, while no reaction was observed with excitation at a wavelength longer than 350 nm, where the molecule still has appreciable absorption. The difference in the photochromic reactivity was attributed to the aggregate formation. From the time-resolved lifetime measurements, the aggregates have a longer lifetime and a longer fluorescence maximum compared with the monomer. Similar characteristic fluorescence properties were observed in the single crystal of **1a**. It is inferred from X-ray crystallographic analysis and polarized fluorescence measurements that the intermolecular interaction between two thiophene rings of neighboring molecules contributes to the aggregate formation.

Acknowledgment. This work was partly supported by Grants-in-Aid for Scientific Research (S) (No. 15105006) and the 21st Century COE Program from the Ministry of Education, Culture, Sports, Science and Technology of Japan. T.F. wishes to thank Research Fellowships of the Japan Society for the Promotion of Science for Young Scientists.

References and Notes

(1) Irie, M. *Photo-Reactive Materials for Ultrahigh-Density Optical Memory*; Elsevier: Amsterdam, The Netherlands, 1994.
(2) Feringa, B. L. *Molecular Switches;* Wiley-VCH: Weinheim, Germany, 2001.
(3) de Silva, A. P. *Electron Transfer in Chemistry*; Vol. 5, Part 1. Molecular-Level Electronics; Wiley-VCH: Weinheim, Germany, 2001.
(4) Irie, M.; Fukaminato, T.; Sasaki, T.; Tamai, N.; Kawai, T. *Nature* **2002**, *420*, 759.
(5) Brown, G. H. *Photochromism*; Wiley-Interscienece: New York, 1971.
(6) Dürr, H.; Bouus-Laurent, H. *Photochromism: Molecules and Systems*; Elsevier: Amsterdam, The Netherlands, 1990.
(7) Irie, M.; Uchida, K. *Bull. Chem. Soc. Jpn.* **1998**, *71*, 985.
(8) Irie, M. *Chem. Rev.* **2000**, *100*, 1685.
(9) Nakamura, S.; Irie, M. *J. Org. Chem.* **1988**, *53*, 6136.
(10) Irie, M.; Lifka, T.; Kobatake, S.; Kato, N. *J. Am. Chem. Soc.* **2000**, *122*, 4871.
(11) Uchida, K.; Nakayama, Y.; Irie, M. *Bull. Chem. Soc. Jpn.* **1990**, *63*, 1311.
(12) Hanazawa, M.; Sumiya, R.; Horikawa, Y.; Irie, M. *J. Chem. Soc., Chem. Commun.* **1992**, 206.
(13) Miyasaka, H.; Arai, S.; Tabata, A.; Nobuto, T.; Mataga, N.; Irie, M. *Chem. Phys. Lett.* **1994**, *230*, 249.
(14) Tamai, N.; Saika, T.; Shimidzu, T.; Irie, M. *J. Phys. Chem.* **1996**, *100*, 4689.
(15) Miyasaka, H.; Nobuo, T.; Itaya, A.; Tamai, N.; Irie, M. *Chem. Phys. Lett.* **1997**, *269*, 281.
(16) Ern, J.; Bens, A. T.; Martin, H.-D.; Mukamel, S.; Schmid, D.; Tretiak, S.; Tsiper, E.; Kryschi, C. *Chem. Phys.* **1999**, *246*, 115.
(17) Shibata, K.; Muto, K.; Kobatake, S.; Irie, M. *J. Phys. Chem. A* **2002**, *106*, 209.
(18) Kobatake, S.; Uchida, K.; Tsuchida, E.; Irie, M. *Chem. Commun.* **2002**, 2804.
(19) Uchida, K.; Irie, M. *Chem. Lett.* **1995**, 969.
(20) Uchida, K.; Ishikawa, T.; Takeshita, M.; Irie, M. *Tetrahedron* **1998**, *54*, 6627.
(21) Uchida, K.; Matsuoka, T.; Kobatake, S.; Yamaguchi, T.; Irie, M. *Tetrahedron* **2001**, *57*, 4559.
(22) Matsuda, K.; Matsuo, M.; Mizoguti, S.; Higashiguchi, K.; Irie, M. *J. Phys. Chem. B* **2002**, *106*, 11218.
(23) Okabe, C.; Tanaka, N.; Fukaminato, T.; Kawai, T.; Irie, M.; Nibu, Y.; Shimada, H.; Goldberg, A.; Nakamura, S.; Sekiya, H. *Chem. Phys. Lett.* **2002**, *357*, 113.
(24) Fukaminato, T.; Kawai, T.; Irie, M. *Proc. Jpn. Acad.* **2001**, *77*, Ser. B, 30.
(25) Yokoyama, Y.; Kurita, Y. *J. Synth. Org. Chem. Jpn.* **1991**, *49*. 364.
(26) Heller, H. G.; Langan, J. R. *J. Chem. Soc., Perkin Trans. 2* **1981**, 341.
(27) Tanaka, N.; Okabe, C.; Sakota, K.; Fukaminato, T.; Kawai, T.; Irie, M.; Goldberg, A.; Nakamura, S.; Sekiya, H. *J. Mol. Strut.* **2002**, *616*, 113.
(28) DiCésare, N.; Belletête, M.; Marrano, C.; Leclerc, M.; Durocher, G. *J. Phys. Chem. A* **1999**, *103*, 795.
(29) Emele, P.; Meyer, D. U.; Holl, N.; Port, H.; Wolf, H. C.; Würthner, F.; Bäuerle, P.; Effenberger, F. *Chem. Phys.* **1994**, *181*, 417.
(30) Halkyard, C. E.; Rampey, M. E.; Kloppenburg, L.; Studer-Martinez, S. L.; Bunz, U. H. F. *Macromolecules* **1998**, *31*, 8655.
(31) Meier, H.; Lehmann, M. *Angew. Chem., Int. Ed.* **1998**, *37*, 643.
(32) Sato, T.; Jiang, D.-L.; Aida, T. *J. Am. Chem. Soc.* **1999**, *121*, 10658.
(33) Levitus, M.; Schmieder, K.; Ricks, H.; Shimizu, K. D.; Bunz, U. H. F.; Garcia-Garibay, M. A. *J. Am. Chem. Soc.* **2001**, *123*, 4259.
(34) Levitus, M.; Zepeda, G.; Dang, H.; Godinez, C.; Khuong, T.-A. V.; Schmieder, K.; Garcia-Garibay, M. A. *J. Org. Chem.* **2001**, *66*, 3188.
(35) Jenekhe, S. A.; Osaheni, J. A. *Science* **1994**, *265*, 765.
(36) Kim, J.; Swager, T. M. *Nature* **2001**, *411*, 1030.
(37) Kim, J.; Levitsky, I. A.; McQuade, D. T.; Swager, T. M. *J. Am. Chem. Soc.* **2002**, *124*, 7710.
(38) Lewis, F. D.; Yang, J.-S. *J. Phys. Chem. B* **1997**, *101*, 1775.
(39) Grabowski, Z. R.; Dobkowski, J. *Pure Appl. Chem.* **1983**, *55*, 245.
(40) Rettig, W. *Angew. Chem., Int. Ed. Engl.* **1986**, *25*, 971.
(41) Irie, M.; Sayo, K. *J. Phys. Chem.* **1992**, *90*, 7671.
(42) Malval, J.-P.; Gosse, I.; Morand, J.-P.; Lapouyade, R. *J. Am. Chem. Soc.* **2002**, *124*, 904.